Supplementary Information

Unique $Cd_{0.5}Zn_{0.5}S/WO_{3-x}$ direct Z-scheme heterojunction with S, O vacancies and twinning superlattices for efficient photocatalytic water-splitting

Teng Hou,[a] Hanchu Chen,[a,c] Yanyan Li,[a] Hui Wang,[a,c] Fengli Yu,[a] Caixia Li,[b] Haifeng Lin,*[a] Shaoxiang Li[b] and Lei Wang[a,b]

[a] *Key Laboratory of Eco-chemical Engineering, Key Laboratory of Optic-electric Sensing and Analytical Chemistry of Life Science, Shandong Provincial Key Laboratory of Olefin Catalysis and Polymerization, Taishan Scholar Advantage and Characteristic Discipline Team of Eco-Chemical Process and Technology, College of Chemistry and Molecular Engineering, Qingdao University of Science and Technology, Qingdao 266042, P. R. China*

[b] *Shandong Engineering Research Center for Marine Environment Corrosion and Safety Protection, College of Environment and Safety Engineering, Qingdao University of Science and Technology, Qingdao 266042, P. R. China*

[c] *Shandong Provincial Key Laboratory of Olefin Catalysis and Polymerization, Key Laboratory of Rubber-Plastics of Ministry of Education, School of Polymer Science and Engineering, Qingdao University of Science and Technology, Qingdao 266042, P. R. China*

* Corresponding author. E-mail address: hflin20088@126.com (H. Lin).

Characterization results

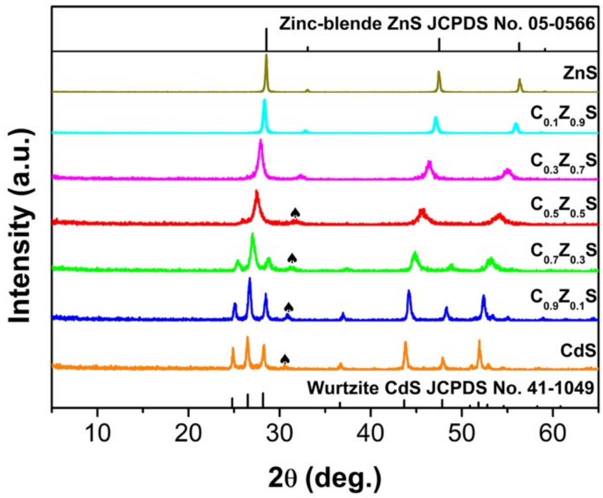

Fig. S1. XRD patterns of the $C_mZ_{1-m}S$ (m = 0, 0.1, 0.3, 0.5, 0.7, 0.9, and 1.0) nanocrystals. The "spade" symbol indicates the zinc-blende CdS (JCPDS card No. 89-0440).

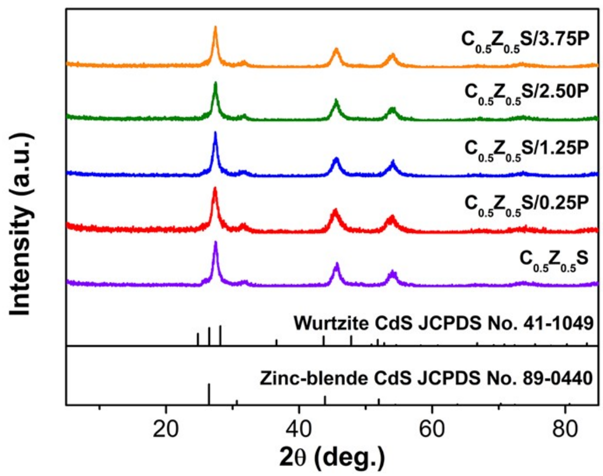

Fig. S2. XRD patterns of $C_{0.5}Z_{0.5}S$ and the $C_{0.5}Z_{0.5}S$/yP synthesized with different $NaH_2PO_2{\cdot}H_2O$ dosages.

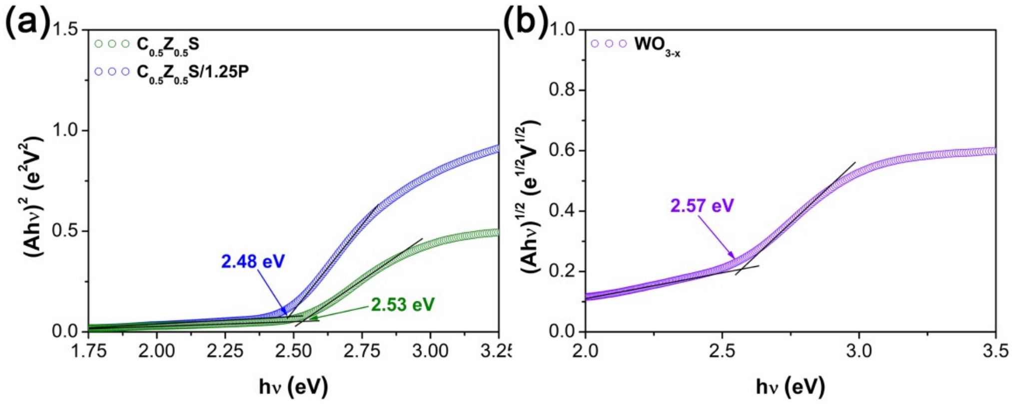

Fig. S3. Determined bandgaps of (a) $C_{0.5}Z_{0.5}S$ and $C_{0.5}Z_{0.5}S/1.25P$ and (b) $WO_{3\text{-}x}$.

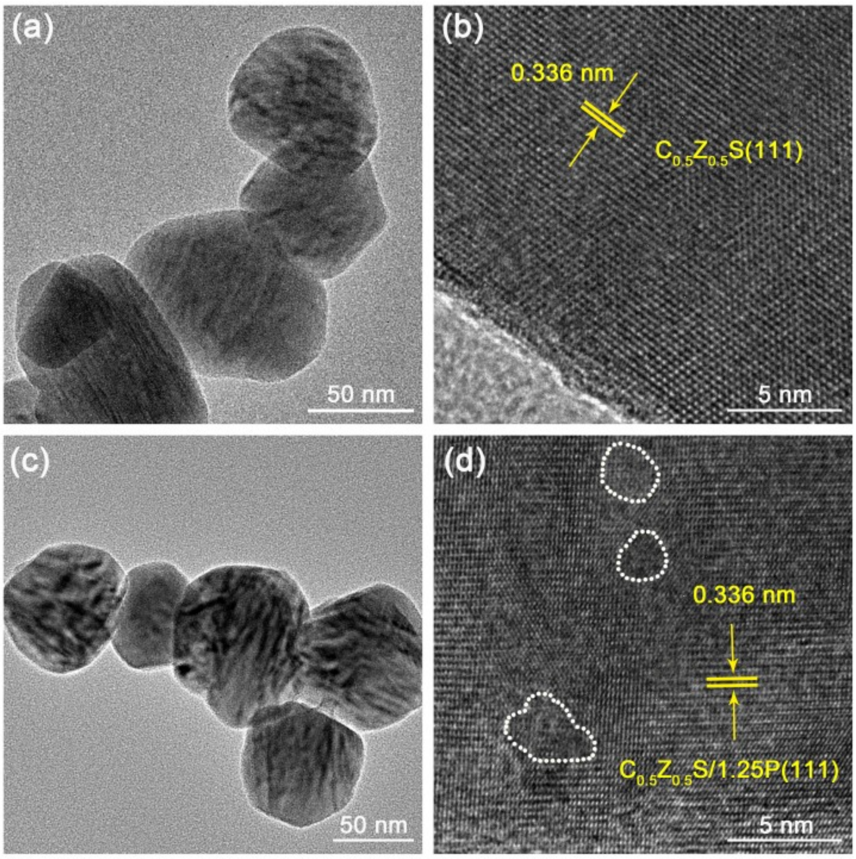

Fig. S4. (a, c) TEM and (b, d) HRTEM images of (a, b) $C_{0.5}Z_{0.5}S$ and (c, d) $C_{0.5}Z_{0.5}S/1.25P$.

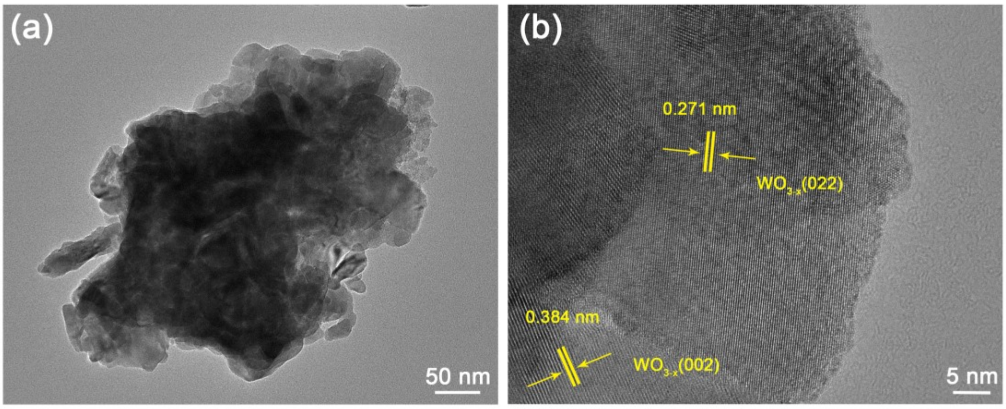

Fig. S5. (a) TEM and (b) HRTEM graphs of WO_{3-x}.

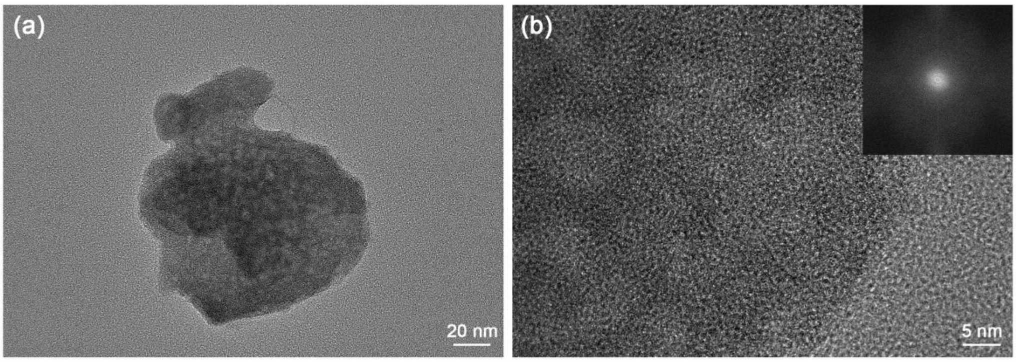

Fig. S6. (a) TEM and (b) HRTEM images of A-WO_{3-x}. The inset in the upper right corner of (b) is the corresponding FFT result.

Table. S1. Elemental compositions of $C_{0.5}Z_{0.5}S$, $C_{0.5}Z_{0.5}S$/1.25P, and $C_{0.5}Z_{0.5}S$/1.25P-7% WO_{3-x} determined by ICP-OES measurement.

Atomic ratios	$C_{0.5}Z_{0.5}S$	$C_{0.5}Z_{0.5}S$/1.25P	$C_{0.5}Z_{0.5}S$/1.25P-7% WO_{3-x}
Cd : Zn : S	1 : 0.94 : 1.90	1 : 0.96 : 1.89	-
Cd : Zn : S : W	-	-	1 : 0.93 : 1.87 : 0.07

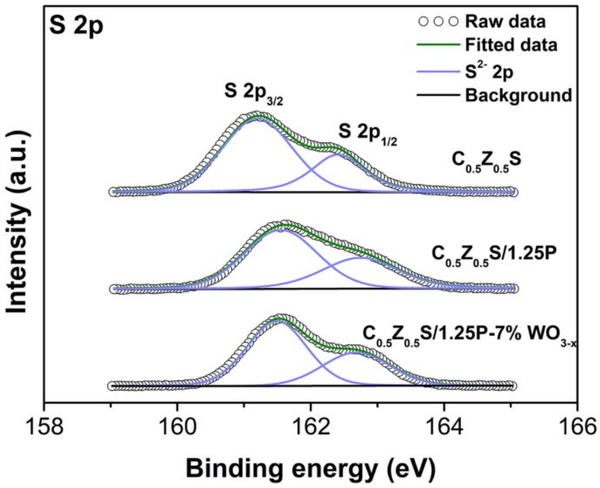

Fig. S7. S 2p XPS spectra of $C_{0.5}Z_{0.5}S$, $C_{0.5}Z_{0.5}S/1.25P$, and $C_{0.5}Z_{0.5}S/1.25P$-7% WO_{3-x}.

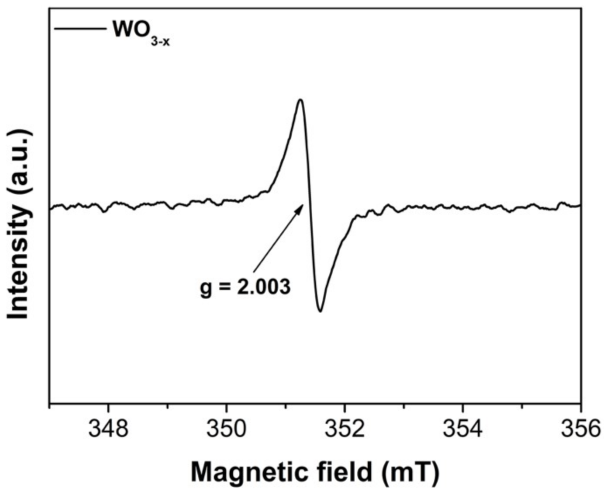

Fig. S8. EPR spectrum of WO_{3-x} nanocrystals.

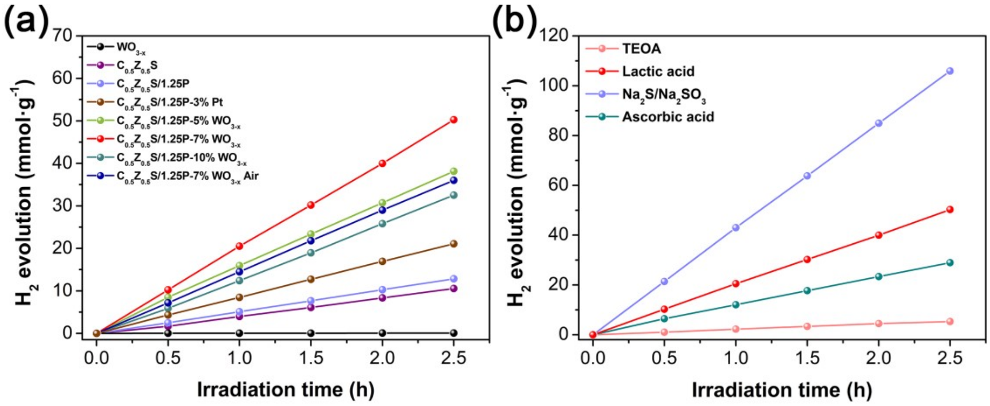

Fig. S9. (a) Photocatalytic HER activities of different samples. (b) The influence of hole scavengers on the HER property of $C_{0.5}Z_{0.5}S/1.25P$-7% WO_{3-x}.

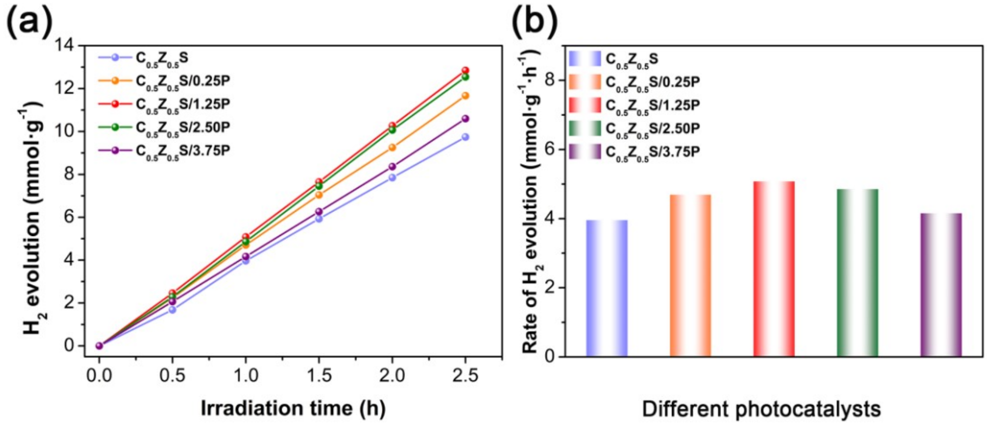

Fig. S10. (a) Photocatalytic HER activities and (b) the corresponding rates of $C_{0.5}Z_{0.5}S$ and $C_{0.5}Z_{0.5}S/yP$ prepared with varying $NaH_2PO_2{\cdot}H_2O$ dosages.

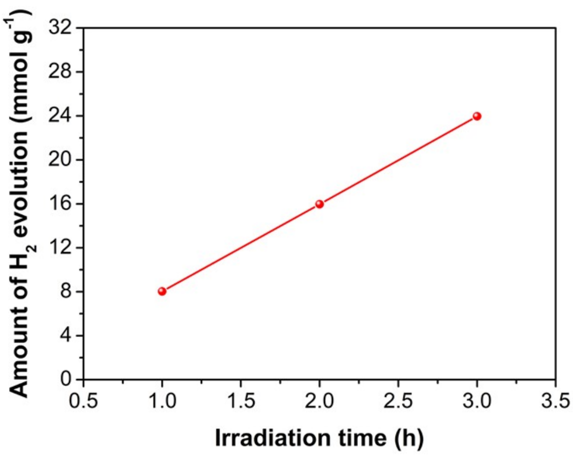

Fig. S11. Photocatalytic H_2 evolution of $C_{0.5}Z_{0.5}S/1.25P\text{-}7\%\ WO_{3-x}$ under 420-nm light irradiation.

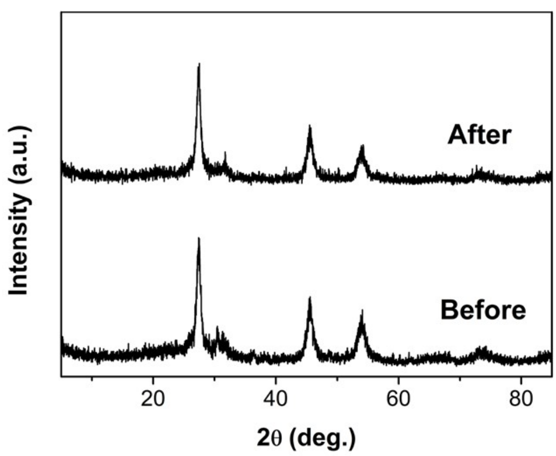

Fig. S12. XRD patterns of the $C_{0.5}Z_{0.5}S/1.25P\text{-}7\%\ WO_{3-x}$ composite before and after photocatalytic stability test.

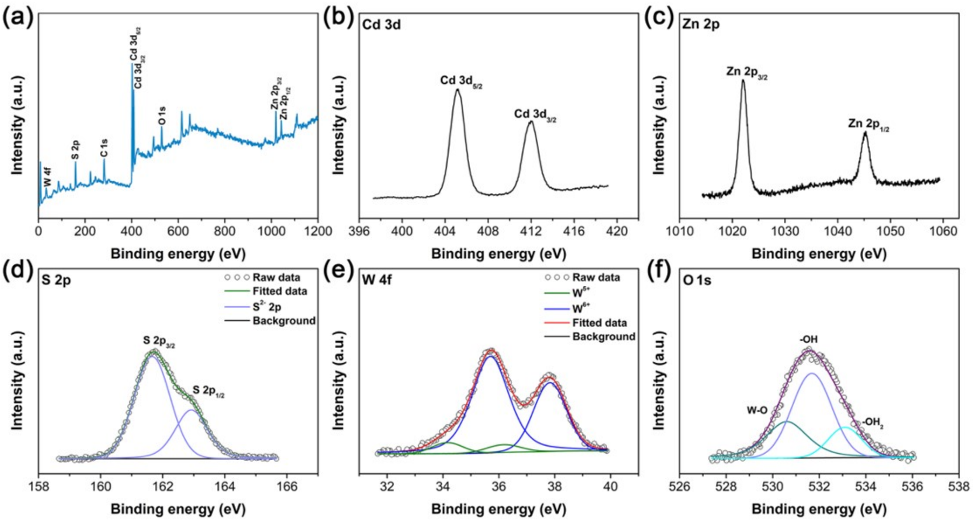

Fig. S13. (a) XPS survey spectrum, (b) Cd 3d, (c) Zn 2p, (d) S 2p, (e) W 4f, and (f) O 1s XPS spectra of the $C_{0.5}Z_{0.5}S$/1.25P-7% WO_{3-x} after cyclic HER test.

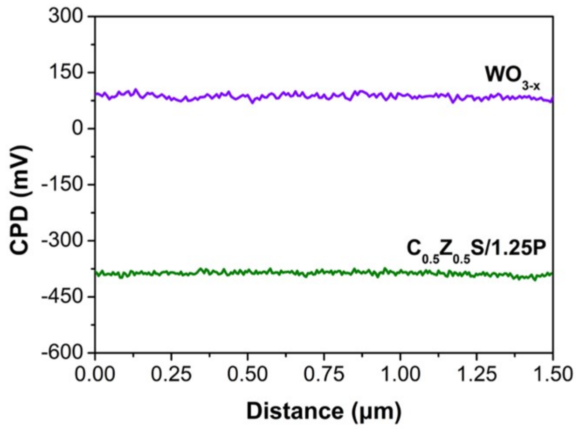

Fig. S14. Contact potential differences of WO_{3-x} and $C_{0.5}Z_{0.5}S$/1.25P in relation to the chromium probe.

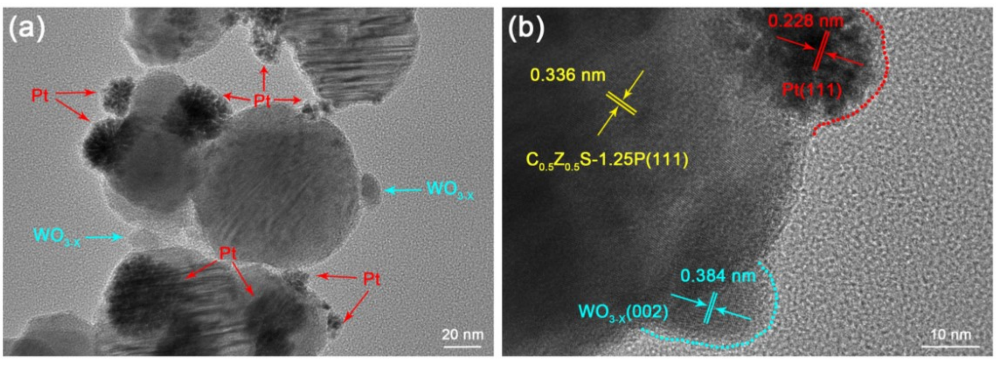

Fig. S15. (a) TEM and (b) HRTEM photographs of the $C_{0.5}Z_{0.5}S$/1.25P-7% WO_{3-x} composite deposited with Pt nanocrystals via visible-light irradiation.

Table. S2. Comparison on the photocatalytic HER activities of WO_3- and CdS-based photocatalysts.

Photocatalyst	Hole scavenger (aqueous solution)	Light source (Xe lamp)	Maximum rate ($mmol \cdot h^{-1} \cdot g^{-1}$)	AQE (420 nm)	Reference
$Cd_{0.5}Zn_{0.5}S/WO_{3-x}$	Lactic acid	λ > 420 nm	20.50	18.0%	This work
$Cd_{0.5}Zn_{0.5}S/WO_{3-x}$	Na_2S/Na_2SO_3	λ > 420 nm	42.97	-	This work
$WO_3/ZnIn_2S_4$	Na_2S/Na_2SO_3	λ > 420 nm	1.95	18.7%	[1]
WO_3/CoP	TEOA	AM 1.5G	4.37	2.0%	[2]
$WO_3@MoS_2$/CdS	Lactic acid	λ > 420 nm	8.20	-	[3]
In_2O_3/CdZnS	Na_2S/Na_2SO_3	λ > 420 nm	1.11	0.3%	[4]
CdS/(WO_3&WS_2)	Lactic acid	λ > 400 nm	0.75	-	[5]
$Cd_{0.5}Zn_{0.5}S$/RP	-	λ > 420 nm	0.14	0.3%	[6]
WS_2/WO_3	Lactic acid	UV-vis light	0.68	-	[7]
WS_2-$WO_3 \cdot H_2O$/g-C_3N_4	Lactic acid	λ > 420 nm	1.28	-	[8]
$Ni_2P/Cd_{0.5}Zn_{0.5}S$	Na_2S/Na_2SO_3	λ > 420 nm	1.31	29.0%	[9]
g-C_3N_4/WO_3	TEOA	AM 1.5G	3.12	-	[10]
$Zn_{0.5}Cd_{0.5}S$/CoP	Ascorbic acid	AM 1.5G	12.18	4.4%	[11]
$WO_3@SnS_2$	Methanol	AM 1.5G	0.13	-	[12]
SiO_2/Ni_2P/rGO/$Cd_{0.5}Zn_{0.5}S$	Na_2S/Na_2SO_3	λ > 420 nm	11.67	15.6%	[13]
Au NPs/$Cd_{0.5}Zn_{0.5}S$	TEOA	λ > 400 nm	12.18	-	[14]
$Cd_{0.5}Zn_{0.5}S/Bi_2S_3$	Na_2S/Na_2SO_3	λ > 400 nm	16.30	19.6%	[15]
$Cd_{0.5}Zn_{0.5}S/BiVO_4$	Na_2S/Na_2SO_3	λ > 420 nm	2.35	24.1%	[16]
$Cd_{0.5}Zn_{0.5}S$/CoO	Na_2S/Na_2SO_3	λ > 420 nm	7.95	37.1%	[17]
$Cd_{0.5}Zn_{0.5}S@Bi_2Fe_4O_9$	Na_2S/Na_2SO_3	λ > 420 nm	0.81	-	[18]
$Cd_{0.5}Zn_{0.5}S/Co_{0.85}Se$	Na_2S/Na_2SO_3	λ > 420 nm	7.59	15.9%	[19]
$Ni(OH)_2/Zn_{0.5}Cd_{0.5}S$	Na_2S/Na_2SO_3	λ > 400 nm	6.87	16.8%	[20]

References:

1 Y. Wang, D. Chen, Y. Hu, L. Qin, J. Liang, X. Sun and Y. Huang, *Sustain. Energy Fuels*, 2020, **4**, 1681-1692.

2 T. Li, X. Guo, L. Zhang, T. Yan and Z. Jin, *Int. J. Hydrogen Energy,* 2021, **46**, 20560-20572.

3 L. Zhang, H. Zhang, C. Jiang, J. Yuan, X. Huang, P. Liu and W. Feng, *Appl. Catal. B: Environ.,* 2019, **259**, 118073.

4 H. Yang, J. Tang, Y. Luo, X. Zhan, Z. Liang, L. Jiang, H. Hou and W. Yang, *Small*, 2021, **17**, 2102307.

5 H. Wang, C. Li, L. Ying and P. Fang, *Appl. Surf. Sci.,* 2018, **448**, 539-546.

6 F. Liu, F. Xue, Y. Si, G. Chen, X. Guan, K. Lu and M. Liu, *ACS Appl. Nano Mater.,* 2021, **4**, 759-768.

7 S. Zhang, S. Chen, D. Liu, J. Zhang and T. Peng, *Appl. Surf. Sci.,* 2020, **529**, 147013.

8 X. Wang, G. Hai, B. Li, Q. Luan, W. Dong and G. Wang, *Chem. Eng. J.,* 2021, **426**, 130822.

9 S. Peng, Y. Yang, J. Tan, C. Gan and Y. Li, *Appl. Surf. Sci.,* 2018, **447**, 822-828.

10 W. Yu, J. Chen, T. Shang, L. Chen, L. Gu and T. Peng, *Appl. Catal. B: Environ.,* 2017, **219**, 693-704.

11 P. Wang, S. Zhan, H. Wang, Y. Xia, Q. Hou, Q. Zhou, Y. Li and R. R. Kumar, *Appl. Catal. B: Environ.,* 2018, **230**, 210-219.

12 X. Zhang, R. Zhang, S. Niu, J. Zheng and C. Guo, *J. Colloid Interface Sci.,* 2019, **554**, 229-238.

13 P. Zhang, C. Xue, Y. Li, S. Guo, X. Zhang, P. Zhang and G. Shao, *Chem. Eng. J.,* 2021, **404**, 126497.

14 Y. Liu, C. Du, C. Zhou and S. Yang, *J. Ind. Eng. Chem.*, 2019, **72**, 338-345.

15 M. Li, J. Sun, B. Cong, S. Yao and G. Chen, *Chem. Eng. J.,* 2021, **415**, 128868.

16 C. Zeng, Y. Hu, T. Zhang, F. Dong, Y. Zhang and H. Huang, *J. Mate. Chem. A,* 2018, **6**, 16932-16942.

17 H. Zhao, L. Guo, C. Xing, H. Liu and X. Li, *J. Mater. Chem. A,* 2020, **8**, 1955-1965.

18 H. Hua, F. Feng, M. Du, Y. Ma, Y. Pu, J. Zhang and X. A. Li, *Appl. Surf. Sci.,* 2021, **541**, 148428.

19 X. Sun, H. Du, *ACS Sustainable Chem. Eng.,* 2019, **7**, 16320-16328.

20 X. Gao, D. Zeng, J. Yang, W. J. Ong, T. Fujita, X. He, J. Liu and Y. Wei, *Chin. J. Catal.,* 2021, **42**, 1137-1146.